Solution Structure of BmKαIT01, an α-Insect Toxin from the Venom of the Chinese Scorpion *Buthus martensii* Karsch[†,‡]

Xiaotian Tong, Jing Zhu, Yuguang Ma, Xiang Chen, Gong Wu, Fahu He, Chunyang Cao, and Houming Wu*

State Key Laboratory of Bio-organic and Natural Products Chemistry, Shanghai Institute of Organic Chemistry, Chinese Academy of Sciences, Shanghai 200032, China

Received April 11, 2007; Revised Manuscript Received July 15, 2007

ABSTRACT: The solution structure of an α-insect toxin from *Buthus martensii* Karsch, BmKαIT01, has been determined by two-dimensional NMR spectroscopy and molecular modeling techniques. Combining the sequence homology comparison and toxicity bioassays, BmKαIT01 has been suggested to be a natural mutant of α-insect toxins and so can serve as a tool to study the relationship of structure−function among this group of toxins. The overall structure of BmKαIT01 shares a common core structure consisting of an α-helix packed against a three-stranded antiparallel *β*-sheet, which exhibits distinctive local conformations within the loops connecting these secondary structure elements. The solution structure of BmKαIT01 features a non-proline *cis* peptide bond between Asn9 and Tyr10, which is proposed to mediate the spatial closing of the five-residue turn (Gln8−Cys12) and the C-terminal segment (Arg58−His64) to form the NC domain and confer the toxin insect-specific bioactivity. Conformational heterogeneity is observed in the solution of BmKαIT01 and could be attributed to the *cis*−*trans* isomerization of the peptide bond between residues 9 and 10. The minor conformation of BmKαIT01 with a *trans* peptide bond between Asn9 and Tyr10 may be responsible for its moderate bioactivity against mammals. The *cis*−*trans* isomerization of the peptide bond between residues 9 and 10 may be the structural basis of dual pharmacological activities of α-insect and α-like scorpion toxins, which is supported by the fact that conformational heterogeneity occurs in the solution structures of LqhαIT, LqqIII, and LqhIII and by comparison of the solution structure of BmKαIT01 with those of some relevant α-type toxins.

Scorpion neurotoxins specially interacting with voltage-gated sodium channels are single-chain peptides composed of 58−76 amino acids cross-linked by four disulfide bridges (*1*). These toxins bind to various receptor sites on the extracelluar face of NaChs[1] and affect their gating properties. Traditionally, they have been divided into two main classes, α- and *β*-toxins, on the basis of their mode of action and binding properties to a distinct receptor site on NaChs (*2*−*4*). The scorpion α-toxins can prolong the action potential by slowing the inactivation of Na^+ currents with no direct effect on activation by binding to site 3 on voltage-dependent NaChs (*5*, *6*). According to their preferential activity to mammals or insects, the α-toxins can be further divided into three subgroups: (1) classical antimammalian toxins, such as Aah II and Lqh II, which are highly toxic to mammals and weakly active on insects, (2) α-toxins highly active on insects (e.g., LqhαIT), which show relatively poor toxicity to mammals, and (3) α-like toxins that act on both insects and mammals (*3*−*9*).

So far, many three-dimensional structures of α-toxins have been determined by NMR or crystallography (*10*−*19*). Most toxins share similar secondary structural elements and globular folding characterized by the presence of a common core consisting of an α-helix packed against a three-stranded antiparallel *β*-sheet. Although the core structures are homologous, they show conformational differences in some regions which are proposed to be responsible for their bioactivity as pointed by Delepierre et al. (*20*). Recently, much attention has been focused on the structure−activity relationship of α-toxins (*21*−*27*), but only the solution structures of α-insect toxins, LqhαIT (*10*) and LqqIII (*11*), are available to date.

BmKαIT01, a toxin from *Buthus martensii* Karsch, was first isolated and characterized by our laboratory and shows a high toxicity toward insects and moderate toxicity against mammals (*28*, *29*). This toxin was considered an α-insect toxin according to sequence similarity and toxicity bioassays. Its crystal structure was resolved by Huang et al. (*30*). By inspection of the crystal structure of the toxin, a non-proline *cis* peptide bond between residues 9 and 10 was identified in the five-residue reverse turn (PDB code 1OMY). On the other hand, the solution conformational study of the typical α-insect toxin, LqhαIT, indicated a *trans* peptide bond in the corresponding position (*10*; PDB code 1LQI). Obviously, these two studies brought puzzles to the conformation of this

[†] This work is supported by the National Science Foundation of China (Grant 20132030) and the Chinese Academy of Sciences (Grant KGCX2-SW-213-05).

[‡] The atomic coordinates of the 20 energy-minimized conformers used to represent the solution structure of BmKαIT01 have been deposited in the Protein Data Bank with the PDB code 2E0H.

* Corresponding author. Tel: 86-21-54925342. Fax: 86-21-64166128. E-mail: hmwu@mail.sioc.ac.cn.

[1] Abbreviations: NaChs, sodium channels; 1D, one dimensional; 2D, two dimensional; 3D, three dimensional; DQF-COSY, double-quantum-filtered shift correlated spectroscopy; NMR, nuclear magnetic resonance; NOESY, nuclear Overhauser enhancement spectroscopy; RMSD, root mean square deviation; TOCSY, total correlation spectroscopy.

10.1021/bi7006788 CCC: $37.00
Published on Web 09/18/2007

peptide bond under physiological conditions. As we know, most peptides exist under physiological conditions as a mixture of more or less well defined, interconverting conformers and a specific receptor select conformer from those already present in solution. The X-ray crystallography provides only a single specific "snapshot" of the structure of a peptide in a crystalline lattice that may be nonrelevant to the biologically active conformer (*31*). The crystal structure of BmKαIT01 well accounts for its antiinsect toxicity but does not for its antimammal activity. Consequently, it is necessary to get further insight into the solution conformation between residues 9 and 10 of α-insect toxins and its relevance to biological activity.

In this paper, NMR spectroscopy and DYANA torsion angle dynamics were employed to investigate the solution structure of BmKαIT01. The results demonstrated that BmKαIT01 exists as a major form with a *cis* peptide bond between amino acids 9 and 10, which was in agreement with the study results of X-ray (*30*). Simultaneously, conformational heterogeneity was observed in the solution of BmKαIT01 and could be attributed to the *cis*−*trans* isomerization of the peptide bond between residues 9 and 10. In addition, the structural basis for the dual bioactivities (antiinsect and antimammal) was discussed on the basis of the topology comparison of the toxin with α-insect toxin LqhαIT, α-like toxin BmK M1, and classic α-toxin Aah II as well.

MATERIALS AND METHODS

NMR Experiments. The isolation and characterization of the peptide BmKαIT01 were reported previously (*28*). The solvents used were either 100% D_2O or a mixture of 90% H_2O and 10% D_2O (v/v). The pH was adjusted to 4.9 by adding 1 μL of dilute DCl or NaOD, and the final concentration was 1.25 mmol/L. The amide proton exchange rate was determined after lyophilization and dissolution in 100% D_2O.

All of the NMR experiments were recorded on a Varian Unity Inova 600 spectrometer. Quadrature detection was employed in all experiments, and the carrier frequency was always maintained at the solvent resonance. Presaturation was used to suppress the water peak in all experiments. 2D DQF-COSY, TOCSY, and NOESY spectra were achieved in the phase-sensitive mode by using the time-proportional phase incrementation method. All 2D NMR spectra were recorded with 4K data points in the t_2 dimension and 512 data points in the t_1 dimension. The TOCSY spectra were recorded using the MLEV-17 pulse sequence with mixing times of 30, 80, and 120 ms. The NOESY spectra were acquired using mixing times of 100, 150, 200, and 300 ms, respectively. To determine slowly exchanging protons, a series of 1D spectra in first 2 h and 2D spectra TOCSY (mixing time 80 ms, 6 h) were recorded at 300 K immediately after the sample was redissolved in 100% D_2O. A shifted sine window function and zero filling were applied prior to Fourier transformation. All experimental data were acquired and processed using the Vnmr 6.1B program on a SUN Sparc Station 4 computer. The processed data were analyzed with XEASY for NMR spectra visualization, peak picking, and peak integration on a Silicon Graphics Indigo R 5000 computer.

Experimental Constraints and Structure Calculation. Most of distance constraints were obtained from the NOESY (150 and 200 ms) spectra in H_2O; additional constraints were from the NOESY (150 ms) spectrum in D_2O. Dihedral angle constraints were derived from $^3J_{HNH\alpha}$ coupling constants, which were obtained by analyses of ^1H NMR and DQF-COSY spectra. In the later calculation, hydrogen bond constraints (revealed by H−D exchange spectra) and the constraints derived from four disulfide bridges (Cys16/Cys36, Cys22/Cys46, Cys26/Cys48, and Cys12/Cys64) were added, where the presence of those constraints was determined on the basis of the geometry of the backbone in the early stage of the calculation. Distance geometry calculations were performed with the target function program DYANA on a Silicon Graphics Indigo II computer. The 35 structures with the lowest constraint violations were subjected to restrained energy minimization (REM) performed with the AMBER 5.0 package. The 20 best conformers with the lowest energy were used to represent the solution conformation of BmKαIT01. The programs PROCHECK and PROCHECK-_NMR were used to evaluate the NMR structures of BmKαIT01. In addition, 3D conformations were produced with the MOLMOL program for visual comparison of the structures on a Silicon Graphics Indigo II computer. For pairs of conformers, RMSD values for various subsets of atoms were calculated.

Molecular Modeling. On the basis of the solution structure of BmKαIT01, the structure model of BmKαIT01 with a *trans* peptide bond between residues 9 and 10 was constructed by deleting the constraints which determine the existence of a *cis* peptide bond, mainly including the characteristic $d_{\alpha\alpha}$ and side-chain/side-chain $d_{\beta\delta}$ NOEs between Asn9 and Tyr10 and the main-chain hydrogen bonds between Tyr10 and His64. The structure model was further subjected to restrained energy minimization (REM) using the AMBER 5.0 package.

RESULTS

NMR Resonance Assignments. The identification of amino acid spin systems and the sequential assignment were done using the standard strategy described by Wüthrich (*32*).

The spin systems of BmKαIT01 were identified on the basis of DQF-COSY and TOCSY spectra recorded with various mixing times in H_2O and D_2O at pH 4.9 and at 300 K. The fingerprint region of the DQF-COSY spectra recorded in H_2O showed most of HN−Hα cross-peaks expected, and then the TOCSY spectra were used to correlate the HN−Hα cross-peaks with their side-chain spin systems for each residue. The spin systems of tyrosine and phenylalanine were assigned by the presence of intraresidual NOE cross-peaks of H_δ to H_β and H_δ to H_α. Likewise, five Asn and one Gln were determined by NOE correlations of NH_δ to H_β and NH_ϵ to H_γ, appearing only in H_2O spectra. Complete identification of amino acid residues for BmKαIT01 was achieved at the stage of sequence-specific assignments.

The spin systems of BmKαIT01 were connected in sequence by virtue of $d_{\alpha N}$ (i, $i+1$), d_{NN} (i, $i+1$), and $d_{\beta N}$ (i, $i+1$) connectivities in well-dispersed NOESY spectra. The possible amino acid types were in good agreement with locations in the peptide on the basis of the known primary structure (Figure 1).

FIGURE 1: Sequence alignments of BmKαIT01 with selected α-toxins. Sequences are aligned according to the cysteine frame. Numbers are labeled with respect to the sequence of BmKαIT01.

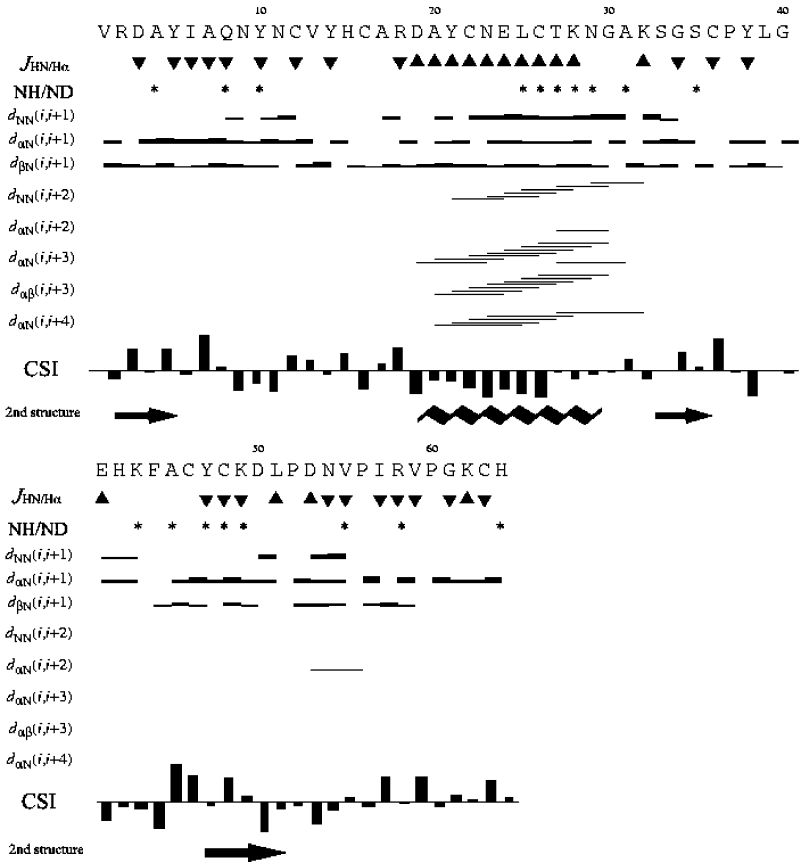

FIGURE 2: Summary of NOE connectivities, *J* coupling constants $^3J_{HN/H\alpha}$, the amide proton exchange rate, and $C^{\alpha}H$ chemical shift index. The thickness of the bar indicates the intensity of NOEs. Asterisks represent the NH protons slowly exchanging. *J* coupling constants $^3J_{HN/H\alpha}$ are smaller than 6.0 Hz (▲) and larger than 9.0 Hz (▼). Positive and negative bars in the chemical shift index (CSI) indicate the $C^{\alpha}H$ protons downfield-shifted and upfield-shifted, respectively, as compared with the $C^{\alpha}H$ proton chemical shifts in random coil. The locations of the second structures found in BmKαIT01 are also indicated.

For BmKαIT01, two amino acid segments that are uniquely present, Asp3-Ala4, Val13-Tyr14, Glu24-Leu25, Leu39-Gly40, and Gly61-Lys62, were used as the starting points for sequential assignments. Starting from the above dipeptide segments, the assignment proceeded smoothly in both forward and reverse directions. Sequential NOE connectivities were observed for all residues of the protein, except Lys43/Phe44. The sequential assignments of four proline residues were obtained on the basis of strong NOE cross-peaks observed between the δ-protons of each proline and the α-protons of the preceding residues and between the α-protons of prolines and the backbone amide protons of the next residues. The summary of sequential and medium-range NOE contacts as well as $^3J_{HNH\alpha}$ coupling constants and amide proton exchange data is presented in Figure 2.

Conformational Heterogeneity of BmKαIT01. In the solution study of BmKαIT01, a series of residues gave two sets of resonances in the TOCSY and DQF-COSY spectra, such

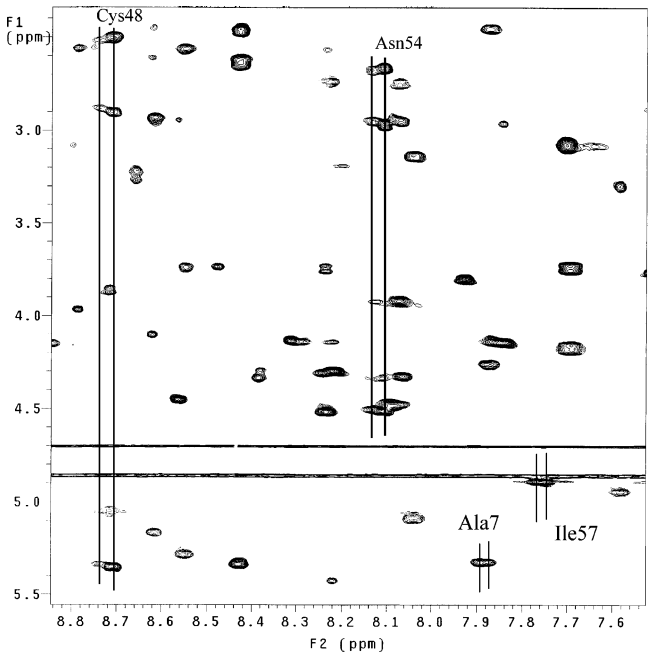

FIGURE 3: Local amplification of the TOCSY spectrum of BmKαIT01 (H_2O, 300 K). The different NH chemical shifts of residues Ala7, Cys48, Asn54, and Ile57 caused by a slow conformational exchange of BmKαIT01 in solution.

as all of the resonances of Ala7, Tyr10, Asn11, Cys36, Ala45, Cys48, Asn54, Ile57, Gly61, and His64 and the aromatic resonances of Tyr5, Tyr14, Tyr47, etc. Figure 3 gave many examples of such observations. No exchange cross-peaks between the two forms were observed in NOESY spectra recorded at 300 or 310 K. The percentage of the two forms was calculated by volume integration especially of the Cys48 HA/HN (Figure 3) and Tyr5 H2,6/H3,5 (not shown) cross-peaks in the NOESY spectra recorded at 300 and 310 K. The population of the minor conformation varied from 20% at 300 K to 26% at 310 K (estimated accuracy ±2%).

Secondary Structure. Secondary structural elements of the toxin were established using the unique NOESY contacts, coupling constants $^3J_{HNH\alpha}$, and hydrogen-bonding pattern characteristic of these structures.

For BmKαIT01, a continuous set of d_{NN} (i, $i + 1$) NOEs were observed in the strand from Asp19 to Lys28, which is indicative of an α-helical structure. The deduction was supported by a series of medium-range NOEs of $d_{\alpha N}$ (i, $i + 3$) and $d_{\alpha\beta}$ (i, $i + 3$). Further corroborative data come from slowly exchanging amide data and $^3J_{HNH\alpha}$ coupling constants: all of the amide protons in the Leu25−Asn29 region are in slow exchange; all of the $^3J_{HNH\alpha}$ coupling constants between residues Asp19−Lys28 are smaller than 7.0 Hz. These data further confirmed our assignment of the above structure as the α-helix. In addition, strands Asp2−Tyr5, Ser33−Ser35, and Tyr47−Leu51 showed strong sequential $d_{\alpha N}$ connectivities and large $^3J_{HNH\alpha}$ (>9.0 Hz) coupling constants. Furthermore, a network of long-range $d_{\alpha N}$, $d_{\alpha\alpha}$, and d_{NN} NOEs were observed for these three strands (Figure 2). These observations suggested the presence of a triple-stranded antiparallel β-sheet. The location of the β-sheet structure was also confirmed by the amide slow exchanging experiments. As shown in Figure 2, all of the amide protons of the central strand were slowly exchanged, whereas the amide protons of two external strands exhibited a typical alternating pattern of rapid and slow exchange rates.

Tight turns of BmKαIT01 are characterized by two medium-to-strong consecutive d_{NN} (i, $i + 1$) interactions, accompanied by weak $d_{\alpha N}$ (i, $i + 2$) NOEs and characteristic patterns of J coupling constants for each type of turn (*32*). Two regular tight turns (Gly40−Lys43 and Pro52−Val55) and a five-residue turn (Gln8−Cys12) were identified by characteristic NOE patterns (Figure 2). However, the classification is rarely possible only on the basis of NOE intensities. In our particular case, small $^3J_{HNH\alpha}$ coupling constants for Glu41 and Asp53 at $i + 1$ positions and large $^3J_{HNH\alpha}$ couplings for His42 and Asn54 at $i + 2$ positions of their respective turns allowed us to classify both Gly40−Lys43 and Pro52−Val55 turns as a type I β-turn. The five-residue turn Gln8−Cys12 was identified on the basis of its characteristic NOEs and hydrogen bond patterns.

Deviations of chemical shifts of Hα protons from their random coil values were suggested to be a useful indicator of secondary structure (*33*−*34*). Commonly, negative deviations for a series of continuous residues are typical of helical structures, whereas positive deviations are indicative of β-sheet. In BmKαIT01, the values of deviation are in good agreement with the helix (Asp19−Lys28) and β-sheet (Arg2−Tyr5, Ser33−Ser35, and Tyr47−Leu51) (seen in Figure 2). These data further confirmed the deduction for the secondary structure of BmKαIT01.

Structure Determination. The input for the distance geometry calculations with the program DYANA consisted of upper distance limits derived from NOESY (mixing time 150 and 200 ms) cross-peak intensities using the program CALIBA, and dihedral angle constraints were obtained from an initial interpretation of the vicinal coupling constants $^3J_{HNH\alpha}$. For the calibration of proton−proton distance limits (r versus the cross-peak intensities), the dependence of $1/r^6$ was used for all protons. The calibration curves were refined by plotting cross-peak volume versus average proton−proton distance according to the preliminary structures. A total of 737 distance constraints were used, which can be clustered into 347 intraresidual, 189 sequential, 66 medium-range ($1 < |i - j| \leq 4$), and 135 long-range ($|i - j| > 4$) NOEs. Thirty-seven ϕ angle constraints ($-55 \pm 15°$ for $^3J_{HNH\alpha} < 6.0$ Hz, $-120 \pm 35°$ for $^3J_{HNH\alpha} \geq 9.0$ Hz, and $-125 \pm 45°$ for 9.0 Hz $> {}^3J_{HNH\alpha} > 8.0$ Hz) were used for structure calculation. In addition, 12 constraints were added for the four-disulfide bonds (three per bond). Eighteen hydrogen bond acceptors were unambiguously identified in the secondary structure elements of the toxin on the basis of slow amide hydrogen exchange data and characteristic NOE patterns (Figure 2). For each hydrogen bond, two limit restraints were used between the NH−O (0.22 nm) and the N−O (0.32 nm) atom pairs. In addition, the program GLOMSA was used to obtain three stereospecific assignments of methylene protons and two isopropyl methyls on the basis of the preliminary structures. In total, 831 constraints (average 13.0 constraints per residue) were obtained and used in the structure calculations for BmKαIT01.

Starting from 200 random structures, 35 preliminary structures with the lowest target functions resulting from distance geometry calculations were subjected to simulated annealing and restrained energy minimization (REM) using the SANDER module of the AMBER 5.0 package. A cutoff radius of 0.8 nm for nonbonded interactions, with a residue-based pair-list routine, was used in all calculations. The force constants for distance restraints in REM were 500 kJ mol^{-1} nm^{-2}. Energy minimization was performed using a combina-

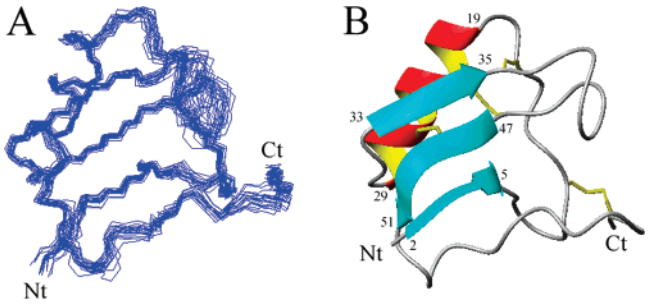

FIGURE 4: Structure of BmKαIT01. (A) Backbone superimposition of the best 20 structures of BmKαIT01. (B) MOLMOL representation of the structure of BmKαIT01 with the lowest energy. Beginning and ending residues of each secondary structural element are labeled according to protein sequence. Nt and Ct indicate N-terminus and C-terminus, respectively.

tion of steepest descent and conjugate gradient algorithms with a gradient convergence norm of less than 10^{-4} kJ mol^{-1} nm^{-1}. After energy minimization with AMBER, the 20 best DYANA conformers with the lowest energy were used to represent the solution conformation of BmKαIT01.

Structure Description. Figure 4A represents the superposition of the polypeptide backbones of the 20 best conformers. No NOE violations larger than 0.30 Å and no angle violations larger than 5° can be found. The overall agreement among individual conformers can be seen by global root mean square deviation (RMSD). The final set of structures of BmKαIT01 displays an overall rmsd of 0.90 Å for the backbone atoms and 1.62 Å for all heavy atoms. The secondary structure is very well defined with RMSD values of 0.22 and 0.39 Å for the backbone atoms of the α-helix and β-sheet residues, respectively. The most poorly defined regions coincide with the Gln8−Cys12 five-residue turn, the Gly40−Lys43 type I β-turn, and the last five C-terminal residues. Analysis of the ensemble of 20 structures using PROCHECK_NMR reveals that 75.1% and 20.9% of the residues lie in the most favored and allowed regions of the Ramachandran ϕ, ψ dihedral angle plot, respectively (plot not shown). The structural statistics for 20 conformers of the toxin are summarized in Table 1.

The structure of BmKαIT01 with the lowest energy is shown in Figure 4B. The overall fold of the toxin BmKαIT01 contains the structural elements characterizing long-chain scorpion α-toxins: a well-organized core formed by an α-helix connected to an antiparallel β-sheet and several loops and turns. The α-helix extends from Asp19 to Lys28 while the β-sheet involves residues Arg2−Tyr5 (strand I), Ser33−Ser35 (strand II), and Tyr47−Leu51 (strand III). Strand II and strand III of the β-sheet are connected by a long loop which is poorly ordered in the structures (Figure 4A). In addition, one tight turn formed by residues Pro52−Val55 and a five-residue turn comprising residues Gln8−Cys12 are also easily recognized in the structure.

DISCUSSION

Comparison of BmKαIT01 to Other Scorpion α-Toxins. To gain further insight into the structural and functional relationships among the α-type toxins, we compared sequence similarity and the structure of BmKαIT01 with some selected toxins. The sequence similarity may be defined with regard to the number of residues, exact matches, or conservative substitutions (Figure 1). BmKαIT01 shares more than 70% identical residues with LqhαIT and LqqIII, the representative α-insect scorpion toxins, whereas the percentage of identity is only about 50−60% with the α-like scorpion toxins and classical scorpion α-toxins, such as BmKM1 and Aah II. Additionally, toxicity bioassays showed that BmKαIT01 is highly toxic to insects, whereas it shows moderate toxicity to mammals (LD_{50}: 0.9 mg/kg in mice) (*29*). On the basis of these facts, BmKαIT01 is proposed to belong to the group of α-insect scorpion toxins.

Table 1: Structural Statistics and Analyses for BmKαIT01

DYANA (35 best structures)	
target function (Å^2)	0.29 ± 0.054
maximum violation (Å)	0.28
maximum violation (deg)	0.04
average no. of upper restraint violations >0.2 Å/structure	0.0
average no. of angle restraint violations >5°/structure	0.0
AMBER (20 best structures)	
total energy (kcal/mol)	−853.63 ± 24.85
bond energy (kcal/mol)	12.66 ± 0.72
angle energy (kcal/mol)	131.82 ± 4.86
dihedral energy (kcal/mol)	120.51 ± 8.38
van der Waals energy (kcal/mol)	−328.70 ± 5.70
eel energy (kcal/mol)	−1741.51 ± 35.18
H bond energy (kcal/mol)	−27.93 ± 1.31
constraint energy (kcal/mol)	6.59 ± 1.22
RMSD from mean coordinates (Å)	
all backbone atoms (Å)	0.90 ± 0.17
all heavy atoms (Å)	1.62 ± 0.22
β-sheet (Å)	0.39 ± 0.10
α-helix (Å)	0.22 ± 0.07
structural analysis (%)	
residues in most favored regions	75.1
residues in allowed regions	20.9
residues in generously allowed regions	3.0
residues in disallowed regions	1.0

Figure 5 shows a best-fit superposition of the backbone conformation of BmKαIT01 with the selected scorpion toxins, including LqhαIT, LqqIII, Aah II, and BmKM1 (*10*,

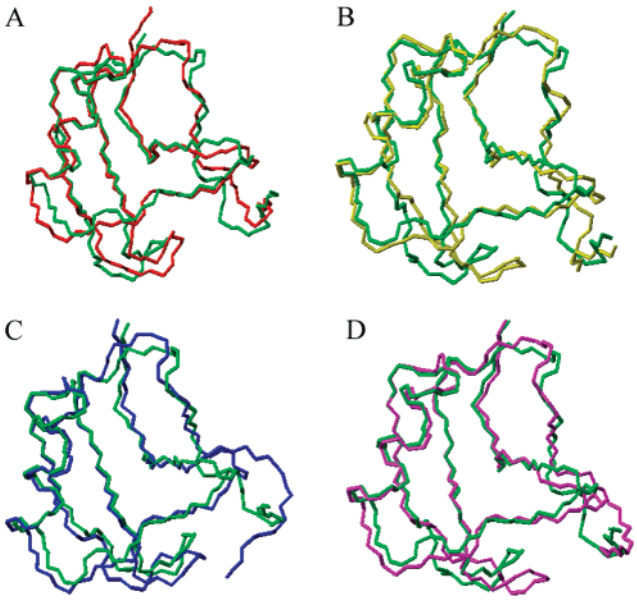

FIGURE 5: Best superposition of backbone structures of BmKαIT01 (green), LqhαIT (A, red), LqqIII (B, yellow), Aah II (C, blue), and BmK M1 (D, magenta). The coordinates of these toxins were obtained from the Protein Data Bank.

11, *15*, *18*). The root mean square deviations (RMSD) calculation was restricted to the backbone atoms of amino acids in secondary structural elements. The toxins and their RMSDs (in parentheses) are LqhαIT (0.71 Å), LqqIII (0.81 Å), Aah II (0.86 Å), and BmKM1 (0.70 Å), respectively. These results reveal that BmKαIT01 has a similar overall fold and shows similar secondary structural elements of other long-chain scorpion toxins. However, it also displays some significant differences in some of the loops and the conformation of C-terminal domain with respect to other toxins of this family.

Main Structural Features of BmKαIT01. The backbone comparison between the above-mentioned toxins clearly highlights the conformational differences in the five-residue turn constituted by residues 8−12 and in the C-terminal domain. The most striking feature occurring in the five-residue turn is a non-proline *cis* peptide bond between residues Asn9 and Tyr10, which is identified on the basis of the characteristic NOEs including $d_{\alpha\alpha}$ and $d_{\beta\delta}$ between residues 9 and 10. The existence of this *cis* peptide bond is further indicated by the upfield chemical shift of the 9β-H (about 0.5 ppm upfield relative to the random coil) due to the C−H π interaction between 9β-H and the aromatic ring of Tyr10 (*35*, *36*). This result coincides with the *cis* bond observed in the crystal structure of BmKαIT01 determined by X-ray crystallography (PDB code 1OMY). This cis peptide bond is stabilized by a pair of main-chain hydrogen bonds between residues Tyr10 and His64 (Tyr10 O−NH His64, His64 O−NH Tyr10) in BmKαIT01

On the other hand, the non-proline cis-peptide bond in the reverse turn of α-like toxins, such as BmKM1/M4, is well documented. In 1999 Wang et al. reported that the non-proline *cis* peptide bond between residues 9 and 10 mediates the closing of the five-residue turn and the C-terminal region to form the NC domain, which is reckoned as the main structural feature in this group of toxins (*18*). This idea is supported recently by structural studies of α-like toxins Lqh III and Lqh6/7 as well (*17*, *37*). Structural comparison between BmKαIT01 and the above α-like toxins showed that the general fold of this part in BmKαIT01 is very similar to that of the α-like toxin BmK M1 (Figure 5D). The non-proline *cis* peptide bond between residues 9 and 10 mediates the spatial closing of the five-residue turn (Gln8−Cys12) and the C-terminal segment (Arg58−His64) to form the NC domain and to form an extending protruding topology in the same way as in α-like toxins. This kind of geometry of the molecule is further validated by the long-range backbone−backbone interactions between the five-residue turn (Gln8−Cys12) and the C-terminal segment (Arg58−His64) deduced from NOESY NMR spectra of BmKαIT01. Simultaneously, the disulfide bond Cys12−Cys63 also contributes to the stability of the NC domain conformation.

However, it is noteworthy that in BmKαIT01 the *cis* peptide bond is formed between residues 9 and 10 in the reverse turn with a non-proline residue at position 9 (designated as nP9-RT), which is distinct from that in α-like toxins, where the *cis* peptide bond is formed between residues 9 and 10 in the reverse turn containing a proline residue at position 9 (designated as P9-RT). According to Wang et al., the occurrence of this *cis* peptide bond is not relevant to the type of residue at position 10 but relevant to the presence of proline at position 9 in BmKM1 and BmKM4 (*18*). Therefore, BmKαIT01 represents as a novel example in the α-toxins: the unique tertiary site RC is formed by the *cis* peptide bond in nP9-RT, because nP9-RT usually leads to a *trans* peptide bond such as that in classical scorpion α-toxins Aah II and BmKM8 demonstrating antimammal activity (*15*, *16*). The presence of a *cis* peptide bond in insect toxins is further proved by the unpublished crystal structure of LqhαIT (*10*).

Conformational Heterogeneity and Mobility. During the NMR study of BmKαIT01, it was found that two sets of parallel resonances in the TOCSY and DQF-COSY spectra could be assigned for a series of residues, which indicates a slow exchange of two conformational isomers of the toxin in solution at the NMR chemical shift time scale. The residues showing conformational exchange involve those in secondary elements, such as Tyr10, Asn11 (in the reverse turn), Ala7, Cys36, Ala45, Cys48 (in the core domain), Asn54, Ile57, Gly61, His64 (in the C-terminus), and especially the aromatic resonances Tyr5, Tyr14, Tyr47, etc. (Figure 3). No exchange cross-peaks between the two forms were observed in NOESY spectra recorded at 300 or 310 K, and the differences of the chemical shifts are all within 0.3 ppm. These observations are very similar to those observed in the typical insect toxin LqhαIT (*10*).

As discussed in the previous section, the solution structure of BmKαIT01 contains a non-proline *cis* peptide bond in its five-residue turn (nP9-RT), which mediates the closing of the five-residue turn and the C-terminal region to form a unique protruding topology of the molecule. Therefore, it is reasonable to relate the conformational mobility of the molecule to the *cis*−*trans* isomerization of the peptide bond, because there is a difference in energy of approximately 2.5 kcal/mol between the *trans* and the *cis* isomers in peptides and proteins (*35*, *36*).

Conformational heterogeneity was also observed in the solution structure of α-like toxins. The NMR studies on the solution structure of LqhIII have previously demonstrated that conformational heterogeneity of the toxin is attributed to the *cis*−*trans* isomeration of the peptide between residues 9 and 10 (*17*, *37*). Therefore, it seems that the *cis*−*trans* peptide bond isomerism between residues 9 and 10 is in common both for α-like toxins and for α-insect toxins, which could be proposed to account for the conformational mobility of these α-insect subfamily scorpion toxins.

Implicated Functional Surfaces of BmKαIT01. Recently, many efforts have been made to explore the functional site of scorpion α-toxins by molecular dissection. In combination with 3D structures determined by NMR or X-ray analysis, the site-directed mutagenesis of antiinsect scorpion α-toxin LqhαIT and α-like toxin BmKM1 has identified the residues important for their bioactivities (*10*, *21*−*27*). These results have revealed that the putative surfaces of α-toxins are mainly composed of (1) the NC domain, including the five-residue turn (residues 8−12) and the C-terminal segment, which determined the specificity of α-toxins and (2) the core domain, including the loop between the β2 and β3 sheet and its adjacent residues, which is suggested to be responsible for the binding with Na^+ channels.

To better understand the molecular basis of the diverse potencies for Na^+ channels of scorpion α-toxins, we compared the residues that were suggested to be involved in the interaction between the toxins and NaChs in LqhαIT

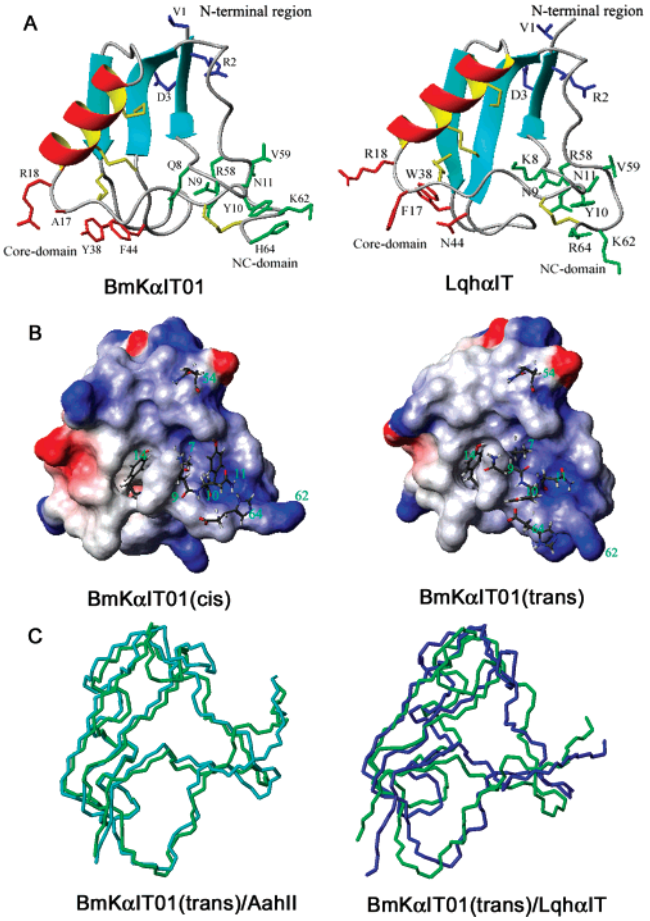

FIGURE 6: (A) Implicated functional surfaces composed with the important residues that are identified by mutagenesis. (B) Comparison of the topology between the BmKαIT01 *cis* conformer and the structural model of the *trans* conformer, where the residues, the resonance frequencies of which are modified by the *cis*−*trans* isomerization, are located. (C) Comparison of the structure model of BmKαIT01 (green) with the *trans* peptide bond between residues 9 and 10 to those of AahII (cyan) and LqhαIT (blue).

and BmKM1 to those in BmKαIT01. As illustrated in Figure 1, the variations mainly occurred in the core domain around residues Ala17 (Phe17 in LqhαIT), Tyr38 (Trp38), His42 (Tyr42), Lys43 (Gly43), and Phe44 (Asn44). Meanwhile, minor differences were observed at residues Gln8 (Lys8) and His64 (Arg64). Further analysis of the 3D structure of BmKαIT01 showed that residues Ala17, Arg18, Tyr38, and Phe44 in the toxin also formed a packed cluster through a series of intramolecular interactions (*9*, *23*, *24*), which may consist of the functional surfaces of BmKαIT01 as the core domain in LqhαIT. On the basis of site-directed mutation studies of LqhαIT and BmKM1, Lys8 or Gln8 was found to be important for their activity and specificity for insects (*23*−*27*). In addition, the important role of the C-terminal His residue was revealed by the increase in the apparent binding and toxicity due to the single N64H mutation in BotIII toxin (*38*). Therefore, the similarity of the functional surfaces (Figure 6A) may well account for their potent toxicity and high specificity to insects.

Moreover, the gene code of BmKαIT01 suggested an amidated C-terminus for the molecule. As previously reported with other toxins C-terminal amidation plays a significant role in toxin recognition of receptor site 3 on voltage-dependent sodium channels. It increased the binding affinity for receptor site 3 on voltage-dependent sodium channels and the toxicity as well. The role of C-terminal amidation has been attributed to that the exchange of an anionic charge for a neutral one at the C-terminus increases the overall positive charge of amidated peptides, which is correlated with their receptor affinities (*39*), while a carboxylated C-terminus may destabilize the toxin−channel complex by electrostatic repulsion (*40*). In BmKαIT01 the amidated C-terminus together with the five-residue reverse turn forms the NC domain of the molecule, which has a protruding topology with the C-terminus extending to solvents (see below and Figure 6B). On the basis of the above discussion, it is tempting to speculate that the amidated C-terminus of the molecule plays a significant role in the toxicity and binding affinity for their sodium channel receptor.

Structural Basis Involved in the Preference for Insect/Mammal Sodium Channels of α*-Toxins.* Mutagenesis analyses have deduced that the NC domain of α-toxins confers their specificity to distinct sodium channels (*23*, *24*, *26*, *27*). On the basis of comparison of the structures of α-type toxins determined by NMR and X-ray, it has been concluded that the α-toxins with the NC domain in a shape that protrudes to solvents appear to have antiinsect activities while the ones having the NC domain as a flat shape exhibit antimammal bioactivities (*24*). Further experimental results indicate that the geometry of the NC domain in α-type toxins is directly linked to the conformation of the peptide bond between residues 9 and 10 (*25*). The *cis* peptide bond between residues 9 and 10 is coupled with the specific hydrogen pattern between the five-residue reverse turn and the C-terminal region, such as the main-chain hydrogen bond between residues 10 and 64, which determines the NC domain in α-toxins protruding to solvents, whereas the same bond with a *trans* conformation makes the NC domain have the flat shape. This result could be further proved by the structure model of BmKαIT01 with a *trans* peptide bond in the corresponding position. Figure 6B demonstrates the topology of the BmKαIT01 *cis* conformer in comparison with the *trans* conformer model, where the residues the resonance frequencies of which are modified by the *cis*−*trans* isomerization were located. It was clear that the conformation of the C-terminus mediated by the *cis* 9,10 bond is closing to the reverse turn and is protruding to the solvent in the *cis* isomer, whereas the C-terminus of the *trans* isomer turns to another side and looks flat. Therefore, the observation of two sets of NMR resonances for residues in the five-residue turn and C-terminus could be attributed to distinct chemical circumstances in these two conformers. Figure 6C further shows the comparison of the structure model of the *trans* conformer with classical mammalian scorpion α-toxin Aah II and antiinsect α-toxin LqhαIT, respectively. The root mean square deviations (RMSD) for the corresponding residues in secondary structure elements are 0.63 Å (Aah II) and 0.80 Å (LqhαIT), indicating the higher similarity of *trans* isomer with the former over the latter. On the basis of the above analyses, BmKαIT01 exists in solution with the *cis* peptide bond between residues 9 and 10 as the main conformation, whereas the *trans* peptide bond in the corresponding position is in the minor conformation, which may well account for its dual bioactivities against insects and mammals. As a result, in α-insect toxins and

α-like toxins, conformational heterogeneity arising from the conformational exchange (*cis*−*trans*) of the peptide bond between residues 9 and 10 is proposed to be the structural basis for their dual bioactivities with high toxicity to insects and moderate toxicity to mammals. Such a mechanism of dynamic conformer selection was well presented in a latest review (*9*), and the solution structure of BmKαIT01 achieved in present studies undoubtedly afforded additional evidence to support the above hypothesis.

In conclusion, as a natural mutant of α-insect toxins, BmKαIT01 shows high toxicity to insect and moderate toxicity to mammal. Structural studies revealed that BmKαIT01 shares a common overall structure of scorpion α-toxins, which is characterized by a hydrophobic core made of an α-helix packed against a three-stranded antiparallel *β*-sheet and several loops extending from the core. Interestingly, it features a non-proline *cis* peptide bond in nP9-RT, which is unique in contrast to that in P9-RT of α-like toxins and the conformational heterogeneity due to the *cis*−*trans* isomerization. Further care was taken in analyzing the relationship between its bioactivity and structural features. By analyses and comparisons of the structures of scorpion α-toxins, it is proposed that the conformation of the peptide bond between residues 9 and 10 is directly linked to the distinct topology of the toxins: the *cis* peptide bond leads to an extending protruded conformation, while the *trans* peptide bond results in a flat geometry. This mechanism might be the structural basis of dual pharmacological activities of α-insect and α-like scorpion toxins.

ACKNOWLEDGMENT

The authors thank the Institute of Molecular Biology and Biophysics, ETH-Hönggerberg, Zürich, Switzerland, for giving the programs DYANA (version 1.5) and XEASY. We are grateful to Prof. Bertini of Florence University, Italy, for giving the program CALIBA and to Prof. James W. Caldwell of California University, CA, for the program AMBER.

REFERENCES

1. Possani, L. D., Becerril, B., Delepierre, M., and Tytgat, J. (1999) Scorpion toxins specific for Na^+-channels, *Eur. J. Biochem. 264*, 287−300.
2. Blumenthal, K. M., and Seibert, A. L. (2003) Voltage-gated sodium channel toxins: poisons, probes, and future promise, *Cell. Biochem. Biophys. 45*, 501−507.
3. Zuo, X. P., and Ji, Y. H. (2004) Molecular mechanism of scorpion neurotoxins acting on sodium channels: insight into their diverse selectivity, *Mol. Neurobiol. 30*, 265−278.
4. Rodriguez de la Vega, R. C., and Possani, L. D. (2005) Overview of scorpion toxins specific for Na^+ channels and related peptides: biodiversity, structure−function relationships and evolution, *Toxicon 46*, 831−844.
5. Goudet, C., Chi, C., and Tytgat, J. (2002) An overview of toxins and genes from the venom of the Asian scorpion *Buthus martensii* Karsch, *Toxicon 40*, 1239−1258.
6. Cestele, S., and Catterall, W. A. (2000) Molecular mechanisms of neurotoxin action on voltage-gated sodium channels, *Biochimie 82*, 883−892.
7. Gordon, D., Martin-Eauclaire, M. F., Cestele, S., Kopeyan, C., Carlier, E., BenKhalifa, R., Pelhate, M., and Rochat, H. (1996) Scorpion toxins affecting sodium current inactivation bind to distinct homologous receptor sites on rat brain and insect sodium channels, *J. Biol. Chem. 271*, 8034−8045.
8. Gordon, D., Gilles, N., Bertrand, D., Molgo, J., Nicholson, G. N., Sauviat, M. P., Shichor, I., Lotan, I., Gurevitz, M., Kallen, R. G., and Heinemann, S. H. (2002) *Perspectives in Molecular Toxinology* (Menez, A., Ed.) Chapter 12, pp 215−238, Wiley and Sons, Chichester, U.K.
9. Gordon, D., Karbat, I., Ilan, N., Cohen, L., Kahn, R., Gilles, N., Dong, K., Stuhmer, W., Tytgat, J., and Gurevitz, M. (2007) The differential preference of scorpion alpha-toxins for insect or mammalian sodium channels: Implications for improved insect control, *Toxicon 49*, 452−472.
10. Tugarinov, V., Kustanovich, I., Zilberberg, N., Gurevitz, M., and Anglister, J. (1997) Solution structure of highly insecticidal recombinant scorpion α-toxin and a mutant with increased activity, *Biochemistry 36*, 2414−2424.
11. Landon, C., Sodano, P., Cornet, B., Bonmatin, J. M., Kopeyan, C., Rochat, H., Vovelle, F., and Ptak, M. (1997) Refined solution structure of the anti-mammal and anti-insect LqqIII scorpion toxin: comparison with other scorpion toxins, *Proteins 28*, 360−374.
12. Pintar, A., Possani, L. D., and Delepierre, M. (1999) Solution structure of toxin 2 from *Centruroides noxius* Hoffmann, a *β*-scorpion toxin neurotoxin acting on sodium channels, *J. Mol. Biol. 287*, 359−367.
13. del Rio-Portilla, F., Hernandez-Marin, E., Pimienta, G., Coronas, F. V., Zamudio, F. Z., de la Vega, R. C., Wanke, E., and Possani, L. D. (2004) NMR solution structure of Cn12, a novel peptide from the Mexican scorpion *Centruroides noxius* with a typical beta-toxin sequence but with alpha-like physiological activity, *Eur. J. Biochem. 271*, 2504−2516.
14. Zhao, B., Carson, M., Ealick, S. E., and Bugg, C. E. (1992) Structure of scorpion toxin variant-3 at 1.2 Å resolution, *J. Mol. Biol. 227*, 239−252.
15. Houset, D., Habersetzer-Rochat, C., Astier, J., and Fontecilla-Camps, J. C. (1994) Crystal structure of toxin II from the scorpion *Androctonus australis* Hector refined at 1.3 Å resolution, *J. Mol. Biol. 238*, 88−103.
16. Li, H. M., Wang, D. C., Zeng, Z. H., Jin, L., and Hu, R. Q. (1996) Crystal structure of an acidic neurotoxin from scorpion *Buthus martensii* Karsch at 1.85 Å resolution, *J. Mol. Biol. 261*, 415−431.
17. Krimml, I., Gilles, N., Sautiere, P., Stankiewicz, M., Pelhate, M., Gordon, D., and Lancelin, J. M. (1999) NMR structures and activity of a novel α-like toxin from the scorpion *Leiurus quinquestriatus hebraeus*, *J. Mol. Biol. 285*, 1749−1763.
18. He, X. L., Li, H. M., Zeng, Z. H., Liu, X. Q., Wang, M., and Wang, D. C. (1999) Crystal structures of two α-like scorpion toxins: non-proline *cis* peptide bonds and implications for new binding site selectively on the sodium channel, *J. Mol. Biol. 292*, 125−135.
19. Li, C., Guan, R. J., Xiang, Y., Zhang, Y., and Wang, D. C. (2005) Structure of an excitatory insect-specific toxin with an analgesic effect on mammals from the scorpion *Buthus martensii* Karsch, *Acta Crystallogr. D61*, 14−21.
20. Lebreton, F., Delepierre', M., Ramirez, A. N., Balderas, C., and Possani, L. D. (1994) Primary and NMR three-dimensional structure determination of a novel crustacean toxin from the venom of the scorpion *Centruroides limpidus limpidus* Karsch, *Biochemistry 33*, 11135−11149.
21. Zilberberg, N., Froy, O., Loret, E., Cestele, S., Arad, D., Gordon, D., and Gurevitz, M. (1997) Identification of structural elements of a scorpion α-neurotoxin important for receptor site recognition, *J. Biol. Chem. 272*, 14810−14816.
22. Sun, Y. M., Bosmans, F., Zhu, R. H., Goudet, C., Xiong, Y. M., Tytgat, J., and Wang, D. C. (2003) Importance of the conserved aromatic residues in the scorpion α-like toxin BmK M1, *J. Biol. Chem. 278*, 24125−24131.
23. Wang, C. G., Gilles, N., Hamon, A., Gall, F. L., Stankiewicz, M., Pelhate, M., Xiong, Y. M., Wang, D. C., and Chi, C. W. (2003) Exploration of the functional site of a scorpion α-like toxin by site-directed mutagenesis, *Biochemistry 42*, 4699−4708.
24. Karbat, I., Frolow, F., Froy, O., Gilles, N., Cohen, L., Turkov, M., Gordon, D., and Gurevitz, M. (2004) Molecular basis of the high insecticidal potency of scorpion alpha-toxins, *J. Biol. Chem. 279*, 31679−31686.
25. Guan, R. J., Xiang, Y., He, X. L., Wang, C. G., Wang, M., Zhang, Y., Sundberg, E. J., and Wang, D. C. (2004) Structural mechanism governing *cis* and *trans* isomeric states and an intramolecular switch for *cis/trans* isomerization of a non-proline peptide bond observed in crystal structures of scorpion toxins, *J. Mol. Biol. 341*, 1189−1204.

26. Liu, L. H., Bosmans, F., Maertens, C., Zhu, R. H., Wang, D. C., and Tytgat, J. (2005) Molecular basis of the mammalian potency of the scorpion α-like toxin BmKM1, *FASEB J. 19*, 594−596.
27. Ye, X., Bosmans, F., Li, C., Zhang, Y., Wang, D. C., and Tytgat, J. (2005) Structural basis for the voltage-gated Na^+ channel selectivity of the scorpion α-like toxin BmKM1, *J. Mol. Biol. 353*, 788−803.
28. Wu, H., Wu, G., Huang, X. L., He, F. H., and Jiang, S. K. (1999) Purification, characterization and structural study of the neuropeptides from scorpion *Buthus martensii* Karsch, *Pure Appl. Chem. 71*, 1157−1162.
29. Wu, H. M., Wu, G., He, F. H., and Jiang, S. K. (1999) A new insect-specific toxin from the venom of scorpion *Buthus martensii* Karsch, *Prog. Nat. Sci. 9*, 631−634.
30. Huang, Y., Huang, Q. C., Chen, H. B., Tang, Y. Q., Miyake, H., and Kusunoki, M. (2003) Crystallization and preliminary crystallographic study of BmKαIT1, a recombinant α-insect toxin from the scorpion *Buthus martensii* Karsch, *Acta Crystallogr. D59*, 1635−1636.
31. Gregory, V. N., and Garland, R. M. (2001) Current developments in computational studies of peptides, *Biopolymers 60*, 77−78.
32. Wüthrich, K. (1986) *NMR of Proteins and Nucleic Acids*, p 292, Wiley, New York.
33. Wishart, D. S., Sykes, B. D., and Richards, F. M. (1991) Relationship between nuclear magnetic resonance chemical shift and protein secondary structure, *J. Mol. Biol. 222*, 311−333.
34. Wishart, D. S., Sykes, B. D., and Richards, F. M. (1992) The chemical shift index: a fast and simple method for the assignment of protein secondary structure through NMR spectroscopy, *Biochemistry 31*, 1647−1651.
35. Jabs, A., Weiss, M. S., and Hilgenfeld, R. (1999) Non-proline *cis* peptide bonds in proteins, *J. Mol. Biol. 286*, 291−304.
36. Pal, D., and Chakrabarti, P. (1999) *Cis* peptide bonds in proteins: residues involved, their conformations, interactions and locations, *J. Mol. Biol. 294*, 271−288.
37. Hamon, A., Gilles, N., Sautiere, P., Martinage, A., Kopeyan, C., Ulens, C., Tytgat, J., Lancelin, J. M., and Gordon, D. (2002) Charaterization of scorpion α-like toxin group using two new toxins from the scorpion *Leiurus quinquestriatus hebraeus*, *Eur. J. Biochem. 269*, 3920−3933.
38. Benkhadir, K., Kharrat, R., Cestèle, S., Mosbah, A., Rochat, H., Ayeb, M. E., and Karoui, H. (2004) Molecular cloning and functional expression of the alpha-scorpion toxin BotIII: pivotal role of the C-terminal region for its interaction with voltage-dependent sodium channels, *Peptide 25*, 151−161.
39. Ferrat, G., Bosmans, F., Tytgat, J., Pimentel, C., Chagot, B., Gilles, N., Nakajima, T., Darbon, H., and Corzo, G. (2005) Solution structure of two insect-specific spider toxins and their pharmacological interaction with the insect voltage-gated Na^+ channel, *Proteins: Struct., Funct., Bioinf. 59*, 368−379.
40. Lebrun, B., Romi-Lebrun, R., Martin-Eauclaire, M-F., Yasuda, A., Ishiguro, M., Oyama, Y., Pongs, O., and Nakajima, T. (1997) A four-disulphide-bridged toxin, with high affinity towards voltage-gated K^+ channels, isolated from *Heterometrus spinnifer* (Scorpionidae) venom, *Biochem. J. 328*, 321−327.

BI7006788